PHYSICAL REVIEW B VOLUME 50, NUMBER 18 1 NOVEMBER 1994-II

Pressure dependence of the magnetic order in $R\mathrm{Mn}_2$ (R=rare earth)

R. Hauser, E. Bauer, E. Gratz, Th. Häufler, G. Hilscher, and G. Wiesinger
Institut für Experimentalphysik, Technische Universität Wien, A-1040 Wien, Austria

(Received 6 April 1994; revised manuscript received 6 July 1994)

Studies of the electrical resistivity were carried out under applied hydrostatic pressure up to 20 kbar and in the temperature range from 1.5 K to room temperature. The heavy $R\mathrm{Mn}_2$ compounds behave significantly differently from those with light rare earths. This is due to the fact that only in the latter case the Mn atoms carry itinerant magnetic moments beyond a critical value of the Mn-Mn distance. Thus in the case of the heavy rare-earth compounds the magnetic order is dominated by the Ruderman-Kittel-Kasuya-Yosida interaction of the rare-earth sublattice, while for the light $R\mathrm{Mn}_2$ compounds the magnetic properties are mainly determined by the itinerant Mn moments. From the influence of pressure on the temperature-dependent resistivity we deduce a change of the interplay between the different kinds of magnetic exchange interactions. As external pressure weakens the itinerant moment a ferromagnetic component is favored within the heavy $R\mathrm{Mn}_2$ compounds. An extraordinary influence of pressure on spin-fluctuation properties has been observed, yielding ($\partial \ln T_{\mathrm{sf}}/\partial p = 75\ \mathrm{Mbar}^{-1}$) for YMn_2.

I. INTRODUCTION

Numerous studies applying a variety of experimental techniques have already been carried out in order to study the peculiar magnetic ordering phenomena in the $R\mathrm{Mn}_2$ compounds, particularly the volume dependence of the magnetic ordering of the Mn sublattice (see, e.g., Refs. 1–21). The compounds form in both the cubic $C15$ (R = Sm, Y, Gd, Tb, Dy, Ho) and the hexagonal $C14$ Laves phase type (R = Pr, Nd, Sm, Ho, Er, Tm). HoMn_2 and SmMn_2 are dimorphous, the structure obtained depending upon heat treatment. In both structures, the Mn atoms lie on the corner of tetrahedra, exhibiting a diamond packing in the cubic case and stacking along chains in the c direction in the hexagonal modification. Since in both structures every Mn atom has six Mn first nearest neighbors, any antiferromagnetic ordering will be highly frustrated. In addition, the instability of the itinerant $3d$ moments leads to unusual magnetic behavior.

Measurements of the thermal expansion[9] have shown that the Mn magnetism is close to instability, leading to huge magnetovolume anomalies. These anomalies are supposed to be associated with a critical distance of the Mn-Mn interatomic distance, $d_c = 2.66$ Å at room temperature, below which the Mn moment is unstable.[11] According to this concept the $R\mathrm{Mn}_2$ series may be classified into four groups, differing in their magnetic behavior. (i) In the case of TmMn_2 and ErMn_2 the Mn-Mn distance is much smaller than d_c and no moment on the Mn site has been observed by NMR measurements.[7] Both compounds are considered as simple ferromagnets.[22] (ii) For compounds containing Dy and Ho (where the Mn-Mn distance is just below the critical value) neutron diffraction measurements yield that only one of four Mn atoms carry a magnetic moment induced by ferromagnetically coupled nearest-neighbor (111) planes of rare-earth moments.[19,21] The value of the induced moment is $0.6\mu_B$ and $1.4\mu_B$, respectively. (iii) In TbMn_2 and in GdMn_2 (the Mn-Mn distance is above d_c) a magnetic moment of $2.4\mu_B$ and $2.6\mu_B$, respectively, is reported to be present on the Mn sites.[7] The magnetic structure is supposed to be a helical antiferromagnet. However, the large volume anomalies observed at T_N are smaller than in YMn_2 with Y considered as a nonmagnetic rare earth. (iv) For the remaining light $R\mathrm{Mn}_2$ compounds a large moment of about $2.7\mu_B$ is found at the Mn sites, which orders antiferromagnetically. At T_N small volume anomalies are observed.[9]

Because of its outstanding properties YMn_2 is a matter of particular interest. Below 92.5 K (on cooling) and 108 K (on warming) the compound undergoes a first-order transition into an antiferromagnetic state with a long wavelength helix accounted for by a propagation vector (0.018,0.003,1) and a Mn moment of $2.8\mu_B$ at 4.2 K.[23] The onset of magnetic order is accompanied by a tetragonal type of distortion of the cubic symmetry.[24] The collapse of the Mn moment yields a 5% shrinking of the cell volume.[2,4] Polarized neutron scattering experiments[13] revealed that at T_N the amplitude of the magnetic Mn moment drops by more than 30% and recovers again with further increasing temperature. Up to $6\,T_N$ strong antiferromagnetic correlations were found to persist, a behavior consistent with Moriya's theory of spin fluctuations.[25,26] Thermal expansion measurements[5] show an anomalously large thermal expansion coefficient (50×10^{-6}/K) above T_N, in accordance with an interpretation in terms of spin-fluctuation theories.[1] Transverse field muon-spin resonance (μSR) measurements show a divergence of the transverse Lorentzian damping rate λ which is attributed to a critical slowing down of longitudinal spin fluctuations. This slowing down is assumed to drive the transition from itinerant towards local moment behavior.[23]

Specific heat studies on paramagnetic

0163-1829/94/50(18)/13493(12)/$06.00

$(Y_{0.97}Sc_{0.03})Mn_2$ (Ref. 8) and $(Y_{0.90}Lu_{0.10})Mn_2$,[27] which provide essential information for the behavior of the paramagnetic state of YMn_2, yield an unusual large electronic specific heat coefficient $\gamma = 140$ mJ/K^2 mol and 120 mJ/K^2 mol, respectively. This finding confirms the occurrence of strong spin fluctuations in the substituted compounds, too. The large values of γ and the transport properties are reminiscent of strongly correlated electron systems. This outstanding behavior may be attributed to the vicinity of antiferromagnetic order, accompanied by large spin fluctuations in combination with frustration of the magnetic moments.[17,18] Resistivity studies above a critical pressure for the suppression of magnetic order should demonstrate whether the above assumptions are valid for the parent compound YMn_2, too.

In the case that the rare earth bears a permanent moment, two types of magnetic ordering are present in these compounds; local rare-earth moments and the itinerant $3d$-electron system of the Mn atoms, which leads to a complex magnetic behavior as can be seen by noncollinear magnetic structures and spin reorientations,[14–16,22] especially for compounds in the vicinity of d_c. Furthermore, they exhibit a transition from an antiferromagnetic type of ordering to a more complex one with an additional ferromagnetic component.[19–22]

Because of the Mn-moment instability, the magnetic properties of $TbMn_2$, YMn_2, and $GdMn_2$ are particularly sensitive to external parameters such as applied pressure,[10,28–35] applied magnetic field,[36] or chemical pressure induced by alloying.[3,11,12,20,37] Small substitutions of about 2–4 % Co and Fe for Mn or Sc for a rare earth, respectively, are sufficient to destabilize the Mn moment. As an example the magnetic state of $TbMn_2$ which is closest to the critical distance is easily transformed by substitution or external magnetic field from a complex antiferromagnetic structure to the same magnetic structure as found in $DyMn_2$ where an induced moment exists only on a part of the Mn-sites. Under ambient conditions the magnetic structure of $TbMn_2$ below T_N is described by two antiferromagnetic phases, denoted as S_1 and S_2, respectively.[20] In $GdMn_2$ measurements under hydrostatic as well as chemical pressure (e.g., substitutions of Gd by Sc) lead to a ferromagnetic type of ordering.[32] Thus it is expected that all the heavy RMn_2 compounds should exhibit the same magnetic structure above a certain critical pressure.

In the present paper a survey of the pressure dependence of various RMn_2 compounds is given. The analysis of the pressure dependence of T_C, T_N, and T_{SR} allows the discussion of the different magnetic interactions (i) between the localized $4f$ moments, (ii) in the rather itinerant $3d$-electron system, and (iii) in the $4f$-$3d$ interaction. This is studied by means of temperature- and pressure-dependent resistivity measurements. According to Matthiessen's rule the electrical resistivity of magnetic materials can be represented by a sum of various contributions:

$$\rho(T) = \rho_0 + \rho_{\mathrm{ph}}(T) + \rho_{\mathrm{mag}}(T), \qquad (1)$$

where ρ_0 represents the temperature-independent residual resistivity, $\rho_{\mathrm{ph}}(T)$ is due to interactions of conduction electrons with thermally excited phonons, and $\rho_{\mathrm{mag}}(T)$ arises from spin-dependent scattering processes. Usually, $\rho_{\mathrm{ph}}(T)$ is best accounted for in the scope of the Bloch-Grüneisen formula yielding a continuous increase with increasing temperature. Thus pronounced anomalies controlled by either pressure or temperature arise only from changes of the magnetic contribution to $\rho(T)$. Both ferromagnetic and antiferromagnetic transitions yield distinct anomalies of $\rho(T)$ and $\partial\rho/\partial T$ vs T. Prominent changes of both quantities are almost identical to the magnetic phase transition temperature as observed from magnetic, thermodynamical, or neutron diffraction measurements. However, $\rho(T)$ data do not always allow one to distinguish between ferro- and antiferromagnetic order. It is therefore necessary to compare the characteristic temperatures deduced from resistivity measurements with those deduced from methods giving the magnetic structure unambiguously.

II. EXPERIMENTAL DETAILS

The samples were prepared from 99.95% pure starting materials by induction melting in a water cooled copper boat. In order to avoid the formation of R_6Mn_{23} the stoichiometry 1:1.93 has been chosen. Note that the choice of the stoichiometry is of essential influence on the physical properties, particular for compounds in the vicinity of the critical distance. The samples were sealed in evacuated (pressure $< 10^{-6}$ mbar) quartz tubes and annealed for one week at a temperature in the range between 1050 K and 1120 K, the exact value depending on the specific rare-earth metal in the sample. The phase purity was examined by x-ray diffraction. Weight losses during melting procedure and heat treatment were found to be around 1% each. While during the melting procedure 98–99 % of the evaporated material consisted of Mn, weight losses during the heat treatment were mainly due to rare earths. The evaporated material was analyzed with a microprobe. Magnetic properties were checked by an ac susceptometer and in a 6 T superconducting quantum interference device (SQUID) magnetometer.

The temperature- and pressure-dependent electrical resistivity has been measured on bar shaped samples in the ranges $1.5\ \mathrm{K} < T < 300\ \mathrm{K}$ and $p < 20$ kbar by means of the common four-probe dc technique. Hydrostatic pressure was generated by a liquid pressure cell, using a 1:4 ethanol-methanol mixture as the pressure transmitting medium.

III. EXPERIMENTAL RESULTS

A. YMn_2 and $LuMn_2$

Figure 1 shows the ρ vs T curves for YMn_2 under various external hydrostatic pressures up to 15.6 kbar. The measurements were started with a value of 4.2 kbar, subsequently the pressure was increased, and finally the

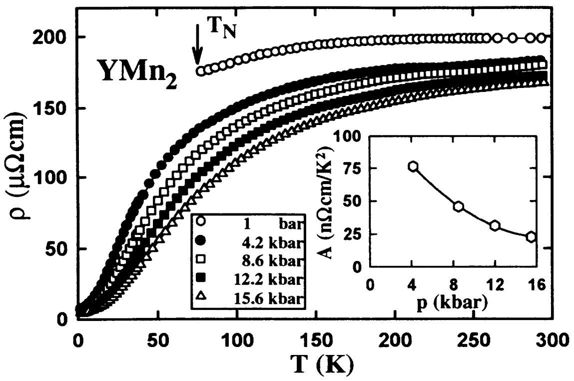

FIG. 1. Temperature-dependent resistivity ρ of YMn_2 at various pressures. The inset shows A vs p of YMn_2.

study has been completed with the measurement at ambient pressure. The arrow in Fig. 1 indicates that point where the sample has been destroyed due to the spontaneous volume expansion at the onset of magnetic order. Measurements performed on a different sample of the same batch yield a critical pressure p_c of about 3 kbar and the initial slope of the pressure derivative of the Néel temperature ($\partial T_N/\partial p$) equals -10 K/kbar.

In the literature there is a wide scatter of data concerning these values. For example, thermal expansion measurements under pressure[10] yield a value of -10 K/kbar, dc susceptibility measurements[28] up to $p = 0.4$ kbar reveal for $\partial T_N/\partial p \simeq -35$ K/kbar, and a value of -40 K/kbar was deduced from an analysis of specific heat data employing the thermodynamical Clausius-Clapeyron relation.[38] Various values for p_c are reported: 1.6 kbar, from specific heat measurements under pressure,[33] 2.7 kbar determined from neutron diffraction measurements under pressure,[31] and 3.7 kbar extrapolated from thermal expansion measurements.[10] The latter two are in reasonable agreement with our data.

The temperature variation of the resistivity of the homologous compound $LuMn_2$ is displayed in Fig. 2. We note that the negative curvature of ρ vs T of $LuMn_2$ is much less pronounced compared to YMn_2.

At low temperatures the electrical resistivity of both compounds can be described satisfactorily by $\rho(T) = \rho_0 + AT^2$. The range of the validity of this expression increases with pressure and with the decrease of the absolute values of A, thus varying from 20 K up to 35 K in the pressure range covered. Spin-fluctuation compounds are characterized by values of A which exceed those of ordinary metals like Cu by several orders of magnitude. The enhanced values of A observed for YMn_2 ($A_{(p=4.2\ \mathrm{kbar})}$ = 80 nΩ cm/K²) and $LuMn_2$ ($A_{(p=1\ \mathrm{bar})}$ 6.4 nΩ cm/K²) thus point to the presence of strong spin fluctuations dominating these compounds. The inset in both figures shows the decrease of the coefficient A with increasing pressure, i.e., the suppression of spin fluctuations due to external pressure. It should be noted that the evaluation of the coefficient A is based on the proper determination of the effective cross section of the samples which can be affected by microcracks or pores. The absolute values of the resistivity are thus given with some uncertainty. However, the relative change of A with pressure does not depend on the real cross section. Comparing the insets in Fig. 1 and Fig. 2 we notice that in the case of $LuMn_2$ A is smaller by at least one order of magnitude and less dependent on pressure.

B. RMn_2 (R = magnetic rare earth)

For R= Tm [Fig. 3(a)] and Er [Fig. 3(b)] the negative curvature of $\rho(T)$ at higher temperature resembles the behavior of $LuMn_2$. The onset of magnetic order is clearly seen by a kink in $\rho(T)$. The value of the ordering temperature as deduced from the maximum slope of

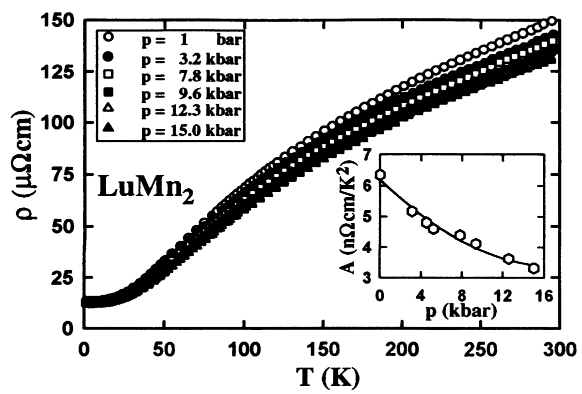

FIG. 2. Temperature-dependent resistivity ρ of $LuMn_2$ at various pressures. The inset shows A vs p of $LuMn_2$.

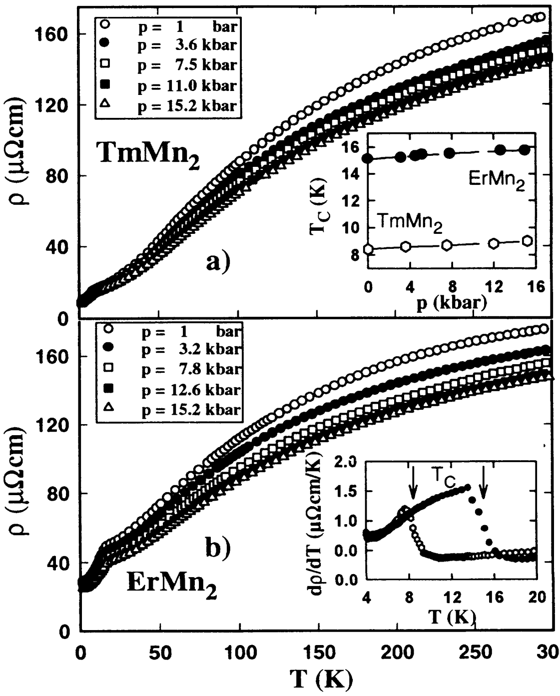

FIG. 3. Temperature-dependent resistivity ρ of (a) $TmMn_2$ and (b) $ErMn_2$ at various pressures. The insets show T_C vs p and $\partial\rho/\partial T$ measured at $p = 1$ bar, respectively.

TABLE I. The magnetic ordering temperatures of the $R\mathrm{Mn}_2$ compounds as deduced from magnetic and resistivity measurements, denoted by the superscripts χ and ρ, respectively. The initial slope of the pressure dependence of Curie and Néel temperatures is taken from a linear fit to the first data points, whereas the critical pressure and critical exponent are derived from a fit of the data to the expression $T_N(p) = T_N(0)(1 - p/p_c)^x$. The magnetic moment μ_{Mn} at the Mn sites is given for comparison.

	T_C^χ (K)	T_C^ρ (K)	$\partial T_C/\partial p$ (K/kbar)	T_N^χ (K)	T_N^ρ (K)	$\partial T_N/\partial p$ (K/kbar)	p_c (kbar)	x	μ_{Mn} (μ_B)
Y				~100	~100	-10[a] to -35[b]	2.7[c]	0.5	2.7[d]
Pr				116	114	-2.9	40.0	1.0	2.8[e]
Nd				101	100	-4.1	22.0	0.9	2.7[e]
Sm				89	89	-5.2	14.0	0.8	2.3[f]
Gd			8.0	106	110	-5.9	11.3	0.6	2.6[g]
Tb	(51)	52	2.0	51	48	-30.0[h]	2.0[h]		2.4[g]
Dy	36	36	1.0						1.4[i]
Ho	23	23	0.5						0.6[j]
Er	15	15	0.07						~ 0[g]
Tm	8	8	0.03						~ 0[g]

[a] From Reference 10.
[b] From Reference 28.
[c] From Reference 31.
[d] From Reference 4.
[e] From Reference 14.
[f] From Reference 6.
[g] From Reference 7.
[h] From Reference 50.
[i] From Reference 19.
[j] From Reference 21.

$\partial\rho/\partial T$ [see inset of Fig. 3(b)] is in good accordance with the Curie temperature T_C found by ac and dc susceptibility measurements (compare Table I). The inset of Fig. 3(a) depicts the pressure dependence of T_C.

In the case of R= Ho [Fig. 4(a)] and Dy [Fig. 4(b)] a continuation of the trend described above is found. However, for DyMn_2 a significant decrease of the resistivity values around T_C with increasing pressure is observable. It should be pointed out that this strong reduction of ρ takes place at temperatures where $\rho(T)$ of YMn_2 is also strongly affected by external pressure. Moreover, the same tendency for saturation is found at elevated temperatures; the absolute resistivity values decrease with rising pressure. Recent powder neutron diffraction measurements indicated a spin reorientation for both HoMn_2 and DyMn_2.[19,21] An inspection of $\partial\rho/\partial T$ for these two compounds reveals a second anomaly below the steep increase ascribed to T_C [see inset of Fig. 4(b)]. However, the value of the spin reorientation temperature T_{SR} cannot be given unambiguously. These anomalies, which are absent in TmMn_2 and ErMn_2, are shifted towards higher temperatures with increasing pressure. As can be seen from the insets of Figs. 3(a) and 4(a), the ordering temperatures for all these heavy $R\mathrm{Mn}_2$ compounds increase with pressure.

At ambient pressure TbMn_2 [Fig. 5(a)] and GdMn_2 [Fig. 5(b)] behave significantly different from the remaining heavy rare-earth compounds. In TbMn_2 at 48 K a phase transition to antiferromagnetic order can unambiguously be determined. Only at $p \geq 1$ kbar can a second phase be clearly resolved, too. An extrapolation to ambient pressures yields a value of 52 K, which we attribute to a transition from the paramagnetic to a ferromagnetic state in accordance with results from various measurements.[20,31] The nature of this transition at ambient pressure and its separation from the close lying first-order transition into an antiferromagnetic state due to the ordering of the Mn moments are still unsettled. From measurements on various samples a critical pressure for the Mn-Mn ordering in the range between 1 and 2 kbar is estimated. This is in accordance with experiments reported previously.[29,31,35] Thus the stability

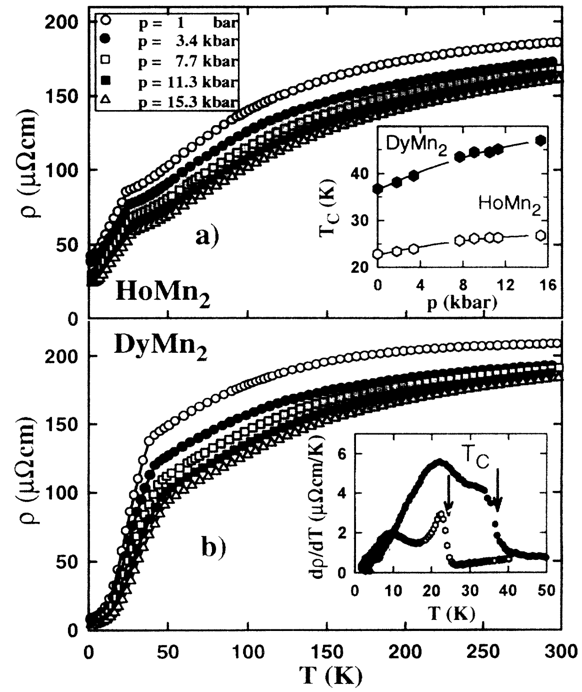

FIG. 4. Temperature-dependent resistivity ρ of (a) HoMn_2 and (b) DyMn_2 at various pressures. The insets show T_C vs p and $\partial\rho/\partial T$ measured at p = 1 bar, respectively.

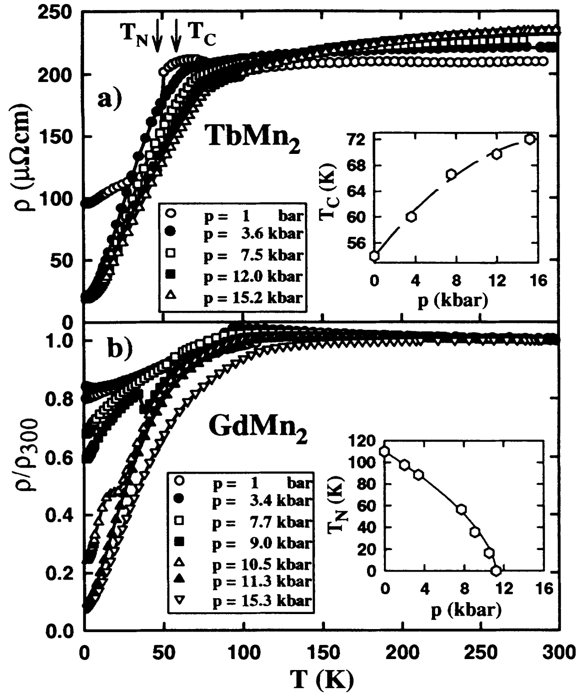

FIG. 5. Temperature-dependent resistivity ρ of (a) TbMn$_2$ and (b) GdMn$_2$ at various pressures. The insets show T_C and T_N vs p of the respective compounds.

of the Mn moment in TbMn$_2$ is particularly sensitive to changes in volume.

As displayed in Fig. 5(a), for $p \geq p_c$ the first-order transition associated with the magnetic order of the Mn sublattice has vanished and the large residual resistivity is considerably reduced. The $\rho(T)$ curves for TbMn$_2$ are now very similar to those measured for DyMn$_2$ shown in Fig. 4(b). T_C can now be resolved more clearly by a kink in ρ vs T.

GdMn$_2$ orders antiferromagnetically at 110 K, a value close to that of YMn$_2$. Note the normalized representation in Figs. 5(b), 6(a), and 6(b), which has been chosen due to the opening of microcracks in the sample when passing through the first-order phase transition. The shift of the discontinuity in $\rho(T)$ towards lower temperatures indicates the decrease of the onset of magnetic order within the 3d-electron subsystem [see also the expanded view given in Fig. 6(a)]. This is connected with the suppression of the intrinsic Mn moment with increasing pressure. The character of the steplike transition changes with pressure: For pressures below about 8 kbar a drop is observed, while for $p \geq 9$ kbar a rise in the resistivity is found, accompanied by a broad hysteresis. From ρ vs T measured at 11.3 kbar no indications for antiferromagnetic order could be determined for temperatures higher than 1.5 K. A fit to the data yields $p_c = 11$ kbar. $\partial T_N/\partial p = -5.9$ K/kbar is in good agreement with the value deduced by Voiron *et al.*[29]

Additionally, for pressures higher than 3 kbar a second magnetic transition in $\rho(T)$ is observed [see the expanded view given in Fig. 6(b) and the inset in Fig. 6(a)].

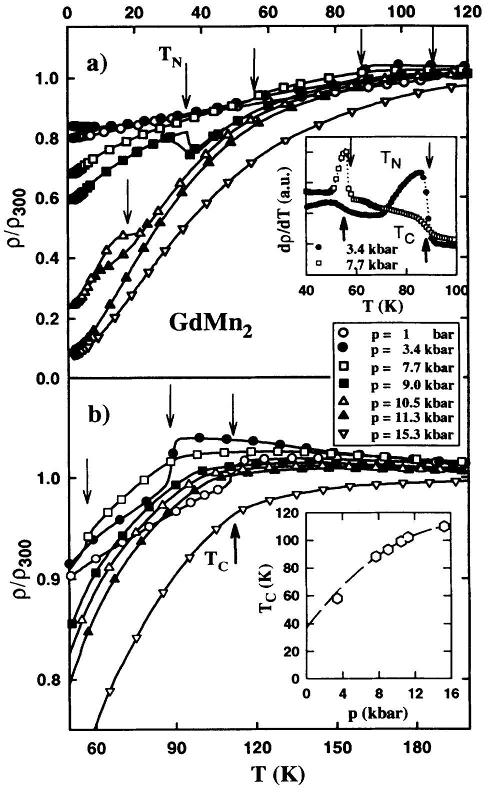

FIG. 6. Temperature-dependent resistivity ρ of GdMn$_2$ at various pressures, given for different expanded views (a) and (b). For the sake of clarity only a fraction of the data points are given as symbols. The insets show $\partial\rho/\partial T$ measured at $p = 3.4$ and 7.7 kbar as well as T_C vs p.

This transition is indicated by a kink in ρ vs T, pointing to a second-order type. It is therefore supposed that under higher pressure GdMn$_2$ orders ferromagnetically by analogy to TbMn$_2$, in accordance with recent magnetization measurements.[32] The inset in Fig. 6(a) depicts $\partial\rho/\partial T$ of GdMn$_2$ for $p = 3.4$ and 7.7 kbar, respectively. These values are just below and above the point where T_N and T_C merge. While T_N is clearly indicated by a cusplike anomaly in the derivative of the resistivity, T_C is found from a steplike change, reminiscent of TmMn$_2$ and ErMn$_2$. Extrapolating T_c vs p towards ambient pressure, indicated by the dashed line in the inset of Fig. 6(b), yields a value of about 8 K/kbar. An estimation of $\partial T_C/\partial p$ above 7.7 kbar, where the second-order transition takes place at higher temperatures than the first-order transition ascribed to Mn-Mn interaction, gives about 2.9 K/kbar. The extrapolated value of T_C towards ambient pressure coincides with the spin reorientation temperature T_{SR} at about 40 K, determined by Mössbauer measurements.[39] Due to the lack of neutron data, the magnetic structure is still under discussion. However, independent of the questions concerning the magnetic structure of the ground state, if we identify T_{SR} with the ordering temperature of the rare-earth sublattice, T_C of GdMn$_2$ exhibits the largest pressure dependence within the RMn$_2$.

A further interesting feature which can be seen in

Figs. 5 and 6 is the change of the slope $\partial\rho/\partial T$ in the paramagnetic regime with increasing pressure, reflecting the suppression of spin fluctuations.

For $SmMn_2$ and $NdMn_2$ the pressure dependence of $\rho(T)$ [Figs. 7(a) and 7(b)] is comparable to that of $GdMn_2$; however, the pressure dependence of T_N differs significantly: Over the whole pressure range covered experimentally, an almost linear behavior is found. Similarly to $GdMn_2$ indications for a second-order phase transition at about 80 K at higher pressures are observed for $SmMn_2$. The value $\partial T_N/\partial p = -4.1$ K/kbar, found for $NdMn_2$, is larger than the results reported by Voiron *et al.*[29] and Kim-Ngan *et al.*,[40] -3.5 K/kbar and -3.45 K/kbar, respectively. For pressures higher than 12 kbar, for both compounds no clear anomaly associated with the ordering of the Mn moments could be detected. The phase transition is supposed to be no longer of first order.

In contrast to $SmMn_2$ and $NdMn_2$ a different temperature variation of the resistivity is found for $PrMn_2$, reminiscent of $LuMn_2$. Besides a discontinuity near T_N, in the whole temperature range $\partial\rho/\partial T > 0$ [Fig. 8(a)], and for $T > 120$ K an almost linear ρ vs T behavior is observed. T_N, indicated by a smooth upturn in ρ vs T, is found to decline in a linear manner over the whole pressure range covered [Fig. 8(b)].

Table I summarizes the ordering temperatures derived from our ac-susceptibility and magnetization measurements as well as from $\partial\rho/\partial T$, and their initial pressure dependences deduced from a linear fit to the data for low pressures. It is to be noted that magnetic and resistivity measurements yield no significant differences in the ordering temperatures. For the heavy R elements (R = Tb, Dy, Ho, Er, and Tm) the maximum of the rather sharp peak of $\chi_{ac}(T)$ has been used to determine T_C since the magnetic transition is already washed out in the dc magnetization in fields as low as 100 Oe. T_N of $GdMn_2$ is hardly resolved in both the dc and ac susceptibility which exhibit only a tiny anomaly at 106 K whilst the specific heat of this specimen exhibits a sharp and symmetric anomaly peaking at 108 K. This and the growth of the magnetization at lower temperatures with a maximum at about 25 K is in agreement with Refs. 3, 22 and 53. It is not unambiguous whether the growing magnetization below 40 K is due to a spin reorientation or associated with the evolution of a ferromagnetic component, since in the specific heat only a broad maximum occurs containing just a small fraction of entropy in comparison to that associated with T_N at 107 K (see also the discussion in Sec. IV B). $SmMn_2$ and $PrMn_2$ exhibit a complex shape of $\chi(T)$ continuously growing down to 89 K and 116 K, respectively, where a sharp drop occurs which is attributed to T_N. At lower temperatures further anomalies can be detected which have been attributed to spin reorientation in the case of $NdMn_2$.[14]

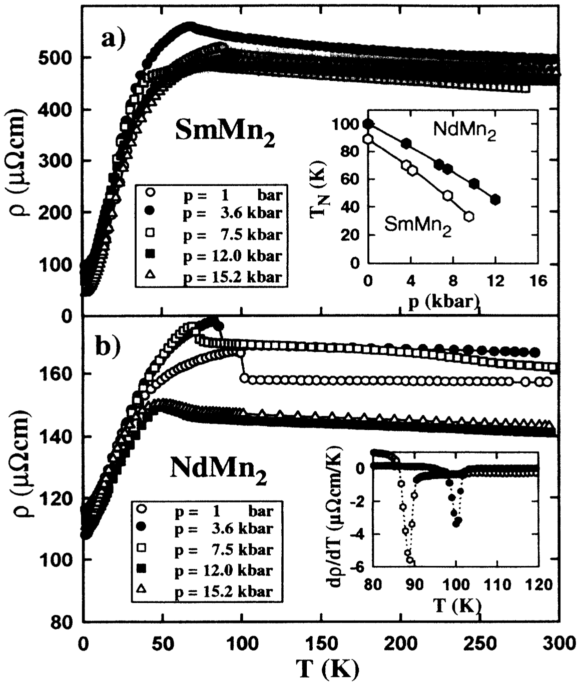

FIG. 7. Temperature-dependent resistivity ρ of (a) $SmMn_2$ and (b) $NdMn_2$ at various pressures. The insets show T_N vs p and $\partial\rho/\partial T$ measured at $p = 1$ bar, respectively.

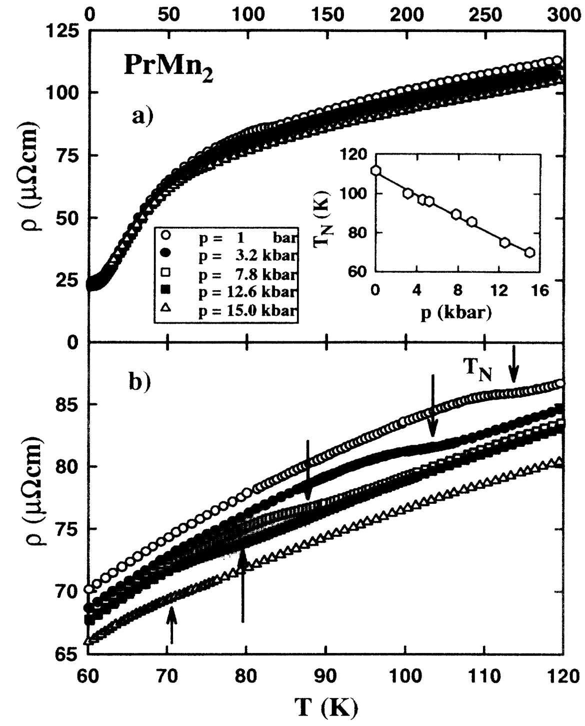

FIG. 8. (a) Temperature-dependent resistivity ρ of $PrMn_2$ at various pressures. The inset shows T_N vs p. (b) The shift of the anomaly in ρ vs T related to T_N with pressure.

The magnetic moment at the Mn sites given in Table I has been taken from the literature. The critical pressure p_c and the exponent x were derived from the expression $T_N(p) = T_N(0)(1 - p/p_c)^x$. Due to the small value of p_c, the exponent x for $TbMn_2$ could not be determined. A significant pressure dependence of the Curie temperature is obtained which obviously increases along with the Mn moment and reaches its maximum in $GdMn_2$ (see also the insets of Figs. 3, 4, 5, and 6). The exponent x and also the critical pressure are found to increase from $GdMn_2$ to $PrMn_2$. In the series of the heavy RMn_2 compounds $\partial T_C/\partial p$ appears to be related to the Mn moment. The exponent x gradually rises from 0.6 to 1 with increasing atomic number of R.

IV. DISCUSSION

A. YMn_2 and $LuMn_2$

The facts that for YMn_2 in the low temperature region all $\rho(T)$ curves for $p > 4$ kbar show a T^2 behavior followed by a pronounced negative curvature in the paramagnetic state (Fig. 1) are typical indications for the occurrence of spin fluctuations. The coefficient A of the T^2 term in the $\rho(T)$ expression, which can be regarded as a measure for the density of states at the Fermi level, is shown as a function of pressure in the inset of Fig. 1. A substantial decrease of A with increasing pressure is observed. Since A is related to the spin fluctuation temperature (T_{sf}) by $T_{sf} = \alpha/\sqrt{A}$,[26,41] this coefficient can be used as a measure for the strength of the spin fluctuations.[42,43] Since there is some uncertainty in defining the pressure-independent constant α we have used the inflection point T_{inf} as a measure of T_{sf}. By analogy with UAl_2,[43] we set $T_{sf} = T_{inf}$, which appears to be justified by the linear relation of $T_{sf}(= T_{inf}) \propto \alpha/\sqrt{A}$ shown in the inset of Fig. 9. Thus we can write the pressure dependence of T_{sf} at 4.2 kbar,

$$\frac{\partial \ln T_{sf}}{\partial p} = \frac{\partial \ln T_{inf}}{\partial p} = \frac{\partial \ln 1/\sqrt{A}}{\partial p} = 75 \text{ Mbar}^{-1}.$$

Furthermore, YMn_2 exhibits a scaling behavior of $\rho(T)$ with T/T_{sf} in an extended temperature range similar to UAl_2 (Fig. 9). This indicates that in these compounds scattering of conduction electrons on spin fluctuations dominates the temperature variation of the resistivity.

The value of $A = 80$ nΩcm/K^2, obtained at $p =$ 4.2 kbar, exceeds that of comparable systems like YCo_2, $ScCo_2$, or $LuCo_2$ by more than one order of magnitude. It is not unlikely that at least a part of the enhanced value of A may be attributed to the frustration of the Mn sublattice. Extrapolating A towards 1 bar (see inset of Fig. 1) yields 160 nΩcm/K^2, a value comparable to that obtained for the classical spin fluctuation system UAl_2 (200 nΩcm/K^2).[43] The pressure response of the resistivity and T_{sf} of YMn_2, however, is substantially larger than that obtained for UAl_2 and UPt_3, with $\partial \ln T_{sf}/\partial p = 24$ Mbar^{-1} and 30 Mbar^{-1}, respectively. The distinct T^2 behavior of the $\rho(T)$ curves in the low temperature range is reminiscent of scattering processes of conduction electrons on heavy quasiparticles in the case of heavy fermion systems. Recently, specific heat measurements under pressure were reported for YMn_2,[33] yielding $\gamma = 168$ mJ/mol K^2 in the proximity of the magnetic instability. This, together with the large magnitude of A and the remarkable similarity to UAl_2, justifies the assumption to classify YMn_2 as a *3d heavy fermion system.*[11] The Kadowaki-Woods plot,[44] displaying the relation between A and γ and being valid for a large number of heavy electron and spin-fluctuation systems, additionally demonstrates that YMn_2 can be included into this category, too.[27]

In $LuMn_2$ the smaller A value and its weaker pressure dependence as well as the less pronounced saturation in ρ vs T are indications that the spin-fluctuation amplitude is in general smaller. However, the proportionality between A and γ^2 ($A/\gamma^2 = 1 \times 10^{-5}$ $\mu\Omega$cm mJ^{-2} mol^2 K^2) is also fulfilled as for YCo_2 and $LuCo_2$ exhibiting less pronounced spin fluctuations. Thus no scaling of $\rho(T)$ with T/T_{sf} can be expected since the phonon and the spin-fluctuation contribution are of comparable size, which is indeed observed.[27]

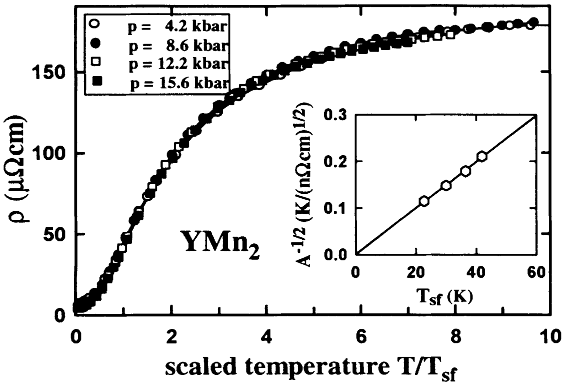

FIG. 9. Temperature- and pressure-dependent resistivity ρ of YMn_2 divided by $T_{sf}(p)$. The inset shows $A^{-1/2}$ vs T_{sf} with pressure as implicit parameter.

B. RMn_2 (R= magnetic rare earth)

The following discussion of the resistivity of the magnetic RMn_2 compounds is based on the validity of Matthiessen's rule [Eq. (1)]. We assume that the phonon-induced resistivity is essentially the same among the entire RMn_2 series; at least it does not show discontinuities in the temperature range under consideration. Consequently, the large variety observed in the ρ vs T behavior throughout the magnetic RMn_2 compounds is supposed to be dominated by the spin-dependent scattering, which is intimately related to the magnetic state of the rare-earth and the Mn ions at a given temperature.

The contribution of localized $4f$ moments to the resistivity, ρ_{mag}, is quite well understand. In the paramagnetic state, ρ_{mag} is temperature independent and proportional to the de Gennes factor [$(g-1)^2 J(J+1)$, where g is the Landé factor and J is the total angular momentum] as long as we can neglect the crystal field influence. This has been proven in the case of several rare-earth intermetallics (RAl_2, RPt, RNi_2, etc.[45]).

In the magnetically ordered state the $4f$ scattering decreases monotonically with decreasing temperature. However, the Mn $3d$ contribution to the spin-dependent scattering depends sensitively on the degree of localization of the Mn $3d$ electrons, as has been shown in the case of $\mathrm{YMn_2}$ and $\mathrm{LuMn_2}$. Since the magnetic state of the Mn moments is a function of both the molecular field of the rare-earth sublattice and the interatomic Mn-Mn distances, resistivity measurements under pressure give important information mainly concerning a change of the magnetic state of the Mn subsystem. In the paramagnetic state the spin-fluctuation contribution to the total resistivity dominates the $4f$ spin disorder scattering. If the magnetic state of the Mn moments is changed as a function of temperature, external pressure, or magnetic field a dramatic change in ρ vs T is expected. This is ascribed to the suppression of spin fluctuations in the $3d$ band. Convincing examples are the resistivity curves of the heavy $R\mathrm{Co_2}$ compounds exhibiting also pronounced spin fluctuations in the paramagnetic state, which are strongly affected by pressure and magnetic field.[27,45]

A first-order transition as, e.g., in some of the $R\mathrm{Co_2}$ compounds gives rise to a pronounced change in resistivity at the corresponding temperature. However, if there is an antiferromagnetic transition we also expect an additional influence due to the appearance of "magnetic" Brillouin zones. This phenomenon is known as the superzone boundary effect, which in principle can give rise to either an increase or a decrease in ρ vs T, depending on how the magnetic Brillouin zones intersect the Fermi surface. The superzone effect was first discussed by Elliott and Wedgewood,[46] for the case of pure rare-earth metals, such as dysprosium.

When passing from $\mathrm{TmMn_2}$ to $\mathrm{PrMn_2}$ a change of the magnetic moment on the Mn sites from almost zero to a more localized moment, via an induced one with a maximum of the spin-fluctuation contribution, takes place. This can also be observed in $\rho(p,T)$, in good accordance with the analysis performed for thermal expansion measurements.[11] Thus, $\rho(p,T)$ reflects the particular dependence of the spin fluctuations on volume and the rare-earth elements involved, as well as their suppression with pressure for $R=$ Tm, Er, Ho, and Dy. In the case of $\mathrm{TbMn_2}$ and $\mathrm{GdMn_2}$ this behavior can clearly be observed for pressures higher than p_c, whereas at ambient pressure it is masked by the first-order transition associated with the effect of localization of the Mn moments and an enhanced residual resistivity below the transition temperature. The variation of the contribution of spin fluctuations to the resistivity can be deduced from the change in the slope of $\partial\rho/\partial T$ which becomes zero or even negative for those $R\mathrm{Mn_2}$ compounds close to d_c ($R=$ Gd and Tb) and once again positive for $\mathrm{PrMn_2}$. The latter compound exhibits the maximum moment on the Mn-sites within the series and is thus closest to the local moment limit.

A prominent case is $\mathrm{GdMn_2}$, where $\partial\rho/\partial T$ above T_N changes sign as a function of pressure showing a maximum negative value for $p = 3.4$ kbar, which points to pronounced spin fluctuations in this pressure interval (Fig. 6). The unusual behavior of $\partial\rho/\partial T$ in the paramagnetic region, which attains even negative values, can be described in the scope of a model developed by Coqblin *et al.*,[41] yielding a particular type of resistivity behavior for compounds close to the magnetic instability. This model has been successfully applied to spin-fluctuation systems based on actinides such as $\mathrm{UAl_2}$ and appears to be valid for the $R\mathrm{Mn_2}$ compounds in the paramagnetic state, too. As mentioned above the discontinuities in ρ vs T near $T = T_N$ are possibly due to the superzone effect. The observed change of the sign of the discontinuity with increasing pressure around 8 kbar for $\mathrm{GdMn_2}$ [see Fig. 6(a)] may be caused by the pressure-induced variation of the magnetic Brillouin zones, thus being responsible for the varying superzone effect. In the same way as the antiferromagnetic order connected with the itinerant Mn-moment is subsequently suppressed, giving way to a rising ferromagnetic component, the spin-dependent scattering of conduction electrons is altered. This can be seen, e.g., in the change of ρ_0, reflecting both the change of conduction electron properties at the Fermi level due to varying magnetic Brillouin zones and the transformation of the magnetic structure to a more simple one.

Beyond the critical pressure, where the antiferromagnetic order is suppressed, the influence of the spin fluctuations in the ordered state is indicated by the negative curvature in ρ vs T. We expect that with further increasing pressure this curvature will flatten out and finally become positive as in the case of the $R\mathrm{Al_2}$ or $R\mathrm{Fe_2}$ compounds, in the same way as pressure reduces the spin fluctuations. Among the family of the $R\mathrm{Fe_2}$ compounds, $\mathrm{CeFe_2}$ is an example where the spin fluctuations cause the same kind of negative curvature.[45]

The key to a deeper understanding of the magnetic properties of the $R\mathrm{Mn_2}$ compounds is the interplay between the variable Mn-Mn interatomic distance and the $4f$-$3d$ interaction among the $R\mathrm{Mn_2}$ series. The latter is solely responsible for the induced $3d$ moments in $R\mathrm{Co_2}$ on the Co sites below T_C. Note that 70 T is enough to induce a Co moment in $R\mathrm{Co_2}$. Thus it is questionable if the concept of a critical Mn-Mn distance, frequently discussed in the literature, is valid as a criterion on its own for the occurrence of a moment on the Mn sites. There are several experimental results contradicting this hypothesis. The most convincing examples with respect to this are compounds of the type $(R_1,R_2)\mathrm{Mn_2}$, where the lattice constant remains significantly above the critical distance; the magnetic order, however, vanishes at a certain concentration.[3,12,47] This is in accordance with the dependence of T_N vs the lattice dimensions, which we qualitatively deduce from converting the applied pressure into lattice constants (Fig. 10), when using the compressibility values at room temperature derived from literature.[31,32] ($\kappa = 4.0, 6.2$, and 3.5 Mbar^{-1} for $\mathrm{TbMn_2}$, $\mathrm{YMn_2}$, and $\mathrm{GdMn_2}$, respectively.) Figure 10 clearly indicates the disappearance of the magnetic order at different Mn-Mn distances. Although there is some uncertainty concerning the lattice parameter at that temperature where the ordering of the Mn sublattice takes place, we believe that this picture is still valid when taking into account the different magnitude of the volume anomalies of the compounds under consideration. Since $\Delta V/V$ at T_N is about 1% for $\mathrm{GdMn_2}$ and 5% for $\mathrm{YMn_2}$, it is reasonable to assume that the Mn moment due to the effect of localization vanishes at different lattice constants for the respective critical pressure.

At least two further important facts have to be con-

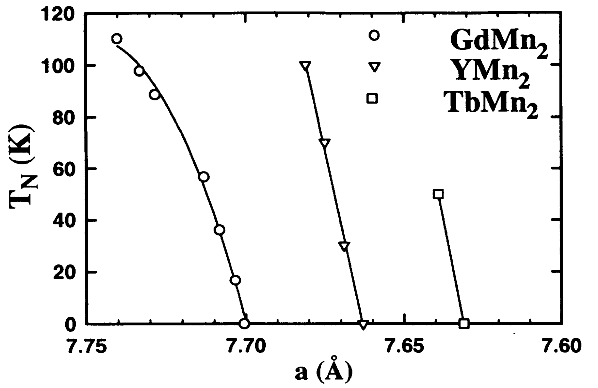

FIG. 10. T_N for TbMn$_2$, YMn$_2$, and GdMn$_2$ as a function of the lattice parameter, converted from pressure when employing $\kappa = 4.0, 6.2$, and 3.5 Mbar^{-1}, respectively.

sidered: (i) the degree of localization, diminishing with increasing atomic number of the rare earth, i.e., decreasing lattice dimensions, and (ii) the impact of the respective molecular field upon the 3*d* subsystem, showing a maximum for *R*= Gd. Thus the interplay of these effects complicates the magnetic and transport properties in particular in the neighborhood of the so-called critical distance.

In order to discuss the pressure dependence of the different magnetic sublattices, i.e., the localized *R*-*R* and the itinerant *d*-*d* subsystems, we display in Figs. 11(a) and 11(b) T_C and T_N at various pressures normalized to the respective ordering temperature at ambient pressure. The gradual suppression of the Mn moment is reflected by the decrease of T_N whilst T_C increases. Supposing that the *R*-*R* interaction of the Ruderman-Kittel-Kasuya-Yosida (RKKY) type is strongly influenced due to the presence of itinerant Mn moments, their suppression leads to a remarkable increase in T_C because of the enhancement of the RKKY interaction [Fig. 11(a)]. An attempt to scale the pressure dependence of T_C with the de Gennes factor valid, e.g., for *R*Al$_2$ (Ref. 48) obviously fails as long as the Mn-Mn interaction is not suppressed in the heavy *R*Mn$_2$ compounds. Thus, the pronounced pressure dependence of T_C (which is much larger than that for the *R*Al$_2$ compounds, e.g., $\partial T_C/\partial p = +0.8$ kbar for GdAl$_2$) points to the presence of a magnetic moment on the Mn sites even in the case of ErMn$_2$, where no moment is detected by NMR.[7] This is in agreement with preliminary results of spin polarized x-ray absorption experiments, which leads to the suggestion that also in ErMn$_2$ a significantly delocalized magnetic moment exists on the Mn sites.[49] As the Mn-Mn interaction is strongly reduced by pressure [Fig. 11(b)] the RKKY interaction rises simultaneously and dominates the magnetic properties. This is evident both from an increase of T_C with pressure and from a scaling of T_C at about 15 kbar (the maximum pressure applied) with the de Gennes factor (Fig. 12). The linear behavior supports the assumption that the magnetic ground state is mainly governed by the RKKY interaction at sufficiently high pressures.

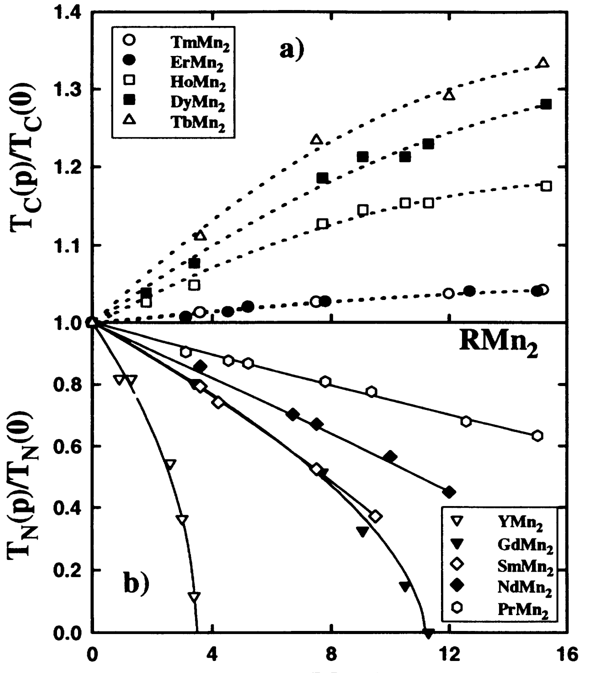

FIG. 11. Pressure dependence of the magnetic ordering temperature for (a) T_C and (b) T_N at various pressures normalized to the respective ordering temperature at ambient pressure. Dotted lines are guides to the eye, whereas full lines are fits according to $T_N(p) = T_N(0)(1-p/p_c)^x$ (the respective exponent x is given in Table I).

While T_C vs p reflects the shift in the competition between the different interactions between the *R* and Mn, T_N vs p allows one to follow the suppression of the moments at the Mn sites and also their change in nature. The variation of the slope of T_N vs p [Fig. 11(b)] alters from a linear to an almost quadratic dependence in the pressure range covered. This follows from the exponent x when proceeding from PrMn$_2$ towards GdMn$_2$, indicating simultaneously a decrease of the magnetic moment at the Mn sites concomitant with an increase of the influence of the spin fluctuations. According to this observation the pressure dependence of T_N changes slope

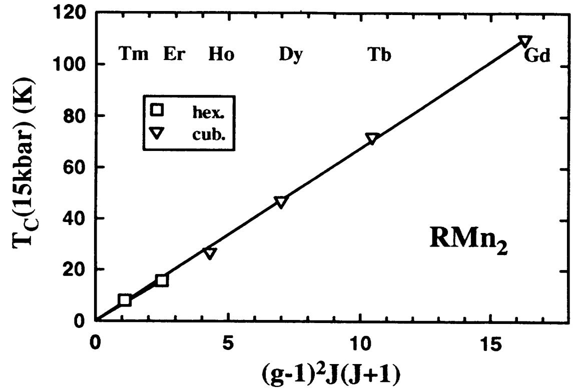

FIG. 12. T_C at maximum applied pressure for the heavy *R*Mn$_2$ compounds vs the de Gennes factor.

when the Mn moment becomes unstable, giving rise to an increase of the spin-fluctuation amplitude.

The most complex situation appears for those compounds where the Mn-Mn distance is just above d_c. Neutron diffraction studies of $TbMn_2$ established the coexistence of two magnetic phases below T_N,[20] S_1 and S_2, and the nonhomogeneous destabilization of the Mn moment under pressure.[31] For pressures above the critical value a single magnetic structure, S_2, is left, which is similar to that of $DyMn_2$. The S_1 phase, described by localized moments on the Mn sites and consequently associated with a larger volume, can also be suppressed by an external field of about 5 T according to magnetostriction measurements.[50] No indication for a structural transition under a field higher than 5 T is found.

A different situation with respect to the field and pressure dependence of T_N seems to appear for YMn_2,[51] $NdMn_2$,[52] and $GdMn_2$.[34] In particular, for the latter magnetostriction measurements in magnetic fields up to 15 T leave the first-order transition associated with the ordering of the Mn moments nearly unaffected, whilst this transition is easily shifted towards lower temperatures by pressure (see Figs. 5, 6, and 7). Since the effects of pressure and external magnetic field upon magnetic phase transitions are thermodynamically related, the first-order transition associated with the magnetovolume effects in these three compounds is more likely of structural origin than due to magnetoelastic effects, in contrast to $TbMn_2$ and presumably the heavy RMn$_2$ compounds where $T_C \geq T_N$.

According to our results the following magnetic phase diagram for $TbMn_2$ and $GdMn_2$ can be drawn (Fig. 13). At ambient pressure and below T_C $TbMn_2$ undergoes a first-order transition at T_N accompanied by a stabilization of a moment at certain Mn sites (S_1 phase). Above a critical pressure of only 2 kbar the Mn moment is suppressed, giving way to a $DyMn_2$-like magnetic structure with T_C increasing with applied pressure. A comparable situation as in $TbMn_2$ seems to appear in $GdMn_2$ above the crossover of T_N and T_C. The anomaly in $\rho(T)$ related to the instability of the Mn moment vanishes at $p_c \approx 11$ kbar. For pressures higher than 3 kbar a kink in ρ vs T points to a second-order transition associated with the Gd sublattice [see also inset of Fig. 6(a)]. This latter anomaly becomes clearly visible above 6 kbar where both transition temperatures merge at about 75 K, in close agreement with recent measurements of low field ac-susceptibility measurements under pressure.[34] For 6 kbar $\leq p \leq p_c$ $GdMn_2$ orders ferromagnetically and subsequently undergoes a transition to an antiferromagnetic state on lowering the temperature. This is reflected by a kink in ρ vs T at higher temperatures and an increase in the resistivity at T_N, accompanied by a broad hysteresis indicating that this transition is still of first order. A separate ordering of the Gd sublattice as proposed by magnetization measurements[22,53] was ruled out by specific heat measurements revealing no distinct anomaly below 50 K.[38] The broad maximum around 40 K in the C_m/T vs T curve is ascribed to the gradual transformation from an antiferromagnetic to a canted state of the Gd moments. However, due to the lack of neutron data the magnetic structure is still under discussion. A noncollinear ferromagnetic ordering of the Gd sublattice below $T_{SR} = 40$ K was suggested by Przewoźnik *et al.*[39] differing from a helical spin structure and a canted ferromagnetic order proposed by Shiga[11] and Okamoto *et al.*,[54] respectively. From our resistivity data we cannot conclude whether the magnetic state of $GdMn_2$ in the pressure interval 6 kbar $\leq p \leq p_c$ is the same as in $TbMn_2$. This will be the subject of further investigations. For pressures higher than the critical pressure $\rho(T)$ of $GdMn_2$ exhibits the same shape as that of $TbMn_2$ under pressure, which indicates that $GdMn_2$ might exhibit a $DyMn_2$-like magnetic structure, too. Magnetization measurements under pressure[32] and NMR measurements performed on $Gd_{0.7}Lu_{0.3}Mn_2$ (Ref. 55) indicate that above p_c $GdMn_2$ behaves similarly to $TbMn_2$ under pressure. However, a comparison of $\rho(T)$ curves of $GdMn_2$ at 15 kbar with those of $DyMn_2$ reveals that spin fluctuations are much more strongly pronounced in the former compound. This we conclude from the distinct negative curvature below T_C. However, at sufficiently high pressures we expect that the spin fluctuations will be suppressed even in $GdMn_2$. In that pressure range all the heavy RMn$_2$ compounds are supposed to be in the same magnetic state.

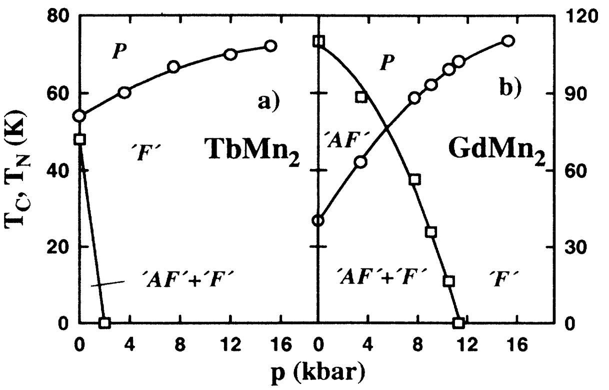

FIG. 13. T_N and T_C as functions of pressure for (a) $TbMn_2$ and (b) $GdMn_2$. "F" denotes a canted ferromagnetic structure as found in $DyMn_2$, whereas "AF" is presumed to be a helical antiferromagnetic structure; see text.

V. CONCLUSION

The temperature variation of the electrical resistivity and its pressure dependence proved to be a proper tool to study the magnetic order within the RMn$_2$ compounds as well as the influence of the spin fluctuation on their physical properties. In particular, we observe for YMn_2, where the antiferromagnetic order can be suppressed for $p \geq 3$ kbar, a large pressure dependence ($\partial \ln T_{sf}/\partial p = 75$ Mbar^{-1}) together with a scaling of $\rho(p,T)$ with T/T_{sf} indicating a suppression of spin fluctuations due to external pressure. Depending on a sensitive interplay among f-f, f-d, and d-d interactions, various magnetic ground states are found among this series. We could show from our measurements that external pressure acts mainly on the itinerant subsystem. Thus, in the same way as the Mn-Mn interaction becomes weaker with growing pressure the RKKY interaction is enforced, yielding a simple ferromagnetic structure, as has been demonstrated for $\mathrm{TbMn_2}$, $\mathrm{GdMn_2}$, and $\mathrm{SmMn_2}$, which match the resistivity behavior of $\mathrm{DyMn_2}$ and $\mathrm{HoMn_2}$. The strong pressure dependence of T_C and T_N can be related to the itineracy of the Mn moments, which are susceptible to changes in volume. Thus the different magnetic and transport properties of the $R\mathrm{Mn_2}$ series has to be seen as a consequence of the interplay of the R molecular field and the degree of itineracy varying with the Mn-Mn distance.

ACKNOWLEDGMENTS

This work was supported by the Austrian FWF, Projects No. 5604 and No. 7608. The authors would like to express their thanks to M. R. Ibarra for providing results prior to publication and to J. Wernisch for microprobe measurements.

---

[1] M. Shiga, J. Phys. Soc. Jpn. **50**, 2573 (1981).
[2] I. Yu Gaidukova and A. S. Markosyan, Fiz. Met. Metalloved **54**, 184 (1982).
[3] I. Yu Gaidukova, S. B. Kruglyashow, A. S. Markosyan, and A. N. Pirogov, Sov. Phys. JETP **57**, 1083 (1983).
[4] Y. Nakamura, M. Shiga, and S. Kawano, Physica B **120**, 212 (1983).
[5] M. Shiga, H. Wada, and Y. Nakamura, J. Magn. Magn. Mater. **31-34**, 119 (1983).
[6] K. Yoshimura and Y. Nakamura, J. Phys. Soc. Jpn. **53**, 3611 (1984).
[7] K. Yoshimura, M. Shiga, and Y. Nakamura, J. Phys. Soc. Jpn. **55**, 3585 (1986).
[8] H. Wada, H. Nakamura, E. Fukami, K. Yoshimura, M. Shiga, and Y. Nakamura, J. Magn. Magn. Mater. **70**, 17 (1987).
[9] H. Wada, H. Nakamura, K. Yoshimura, M. Shiga, and Y. Nakamura, J. Magn. Magn. Mater. **70**, 134 (1987).
[10] G. Oomi, T. Terada, M. Shiga, and Y. Nakamura, J. Magn. Magn. Mater. **70**, 137 (1987).
[11] M. Shiga, Physica B **149**, 293 (1988).
[12] I. Yu Gaidukova, I. S. Dubenko, R. Z. Levitin, A. S. Markosyan, and A. N. Pirogov, Sov. Phys. JETP **67**, 2522 (1988).
[13] T. Freltoft, P. Böni, G. Shirane, and K. Motoya, Phys. Rev. B **37**, 3454 (1988).
[14] R. Ballou, J. Deportes, R. Lemaire, and B. Ouladdiaf, J. Appl. Phys. **63**, 3487 (1988).
[15] S. Labroo, N. Ali, and P. Robinson, J. Appl. Phys. **67**, 5292 (1990).
[16] S. Labroo, F. Williams, and N. Ali, J. Appl. Phys. **67**, 5295 (1990).
[17] R. Ballou, J. Deportes, and M. D. Núñez-Regueiro, Phys. Rev. Lett. **66**, 1910 (1991).
[18] M. D. Núñez Regueiro, C. Lacroix, and R. Ballou, Phys. Rev. B **46**, 990 (1992).
[19] C. Ritter, S. H. Kilcoyne, and R. Cywinski, J. Phys. Condens. Matter **3**, 727 (1991).
[20] P. J. Brown, B. Ouladdiaf, R. Ballou, J. Deportes, and A. S. Markosyan, J. Phys. Condens. Matter **4**, 1103 (1992).
[21] C. Ritter, R. Cywinski, S. H. Kilcoyne, and S. Mondal, J. Phys. Condens. Matter **4**, 1559 (1992).
[22] Y. Makihara, Y. Andoh, Y. Hashimoto, H. Fujii, M. Hasuo, and T. Okamoto, J. Phys. Soc. Jpn. **52**, 629 (1983).
[23] R. Cywinski, S. H. Kilcoyne, and C. A. Scott, J. Phys. Condens. Matter **3**, 6473 (1991).
[24] I. Yu. Gaidukova, V. V. Kelarev, A. S. Markosyan, A. Z. Menshikov, and A. N. Pirogov, J. Magn. Magn. Mater. **72**, 357 (1988).
[25] T. Moriya, J. Magn. Magn. Mater. **14**, 1 (1979).
[26] T. Moriya, *Spin Fluctuations in Itinerant Electron Magnetism* (Springer, Berlin, 1985).
[27] R. Hauser, Ph.D. thesis, T.U. Vienna, 1994.
[28] B. Ouladdiaf, Ph.D. thesis, Grenoble, 1986.
[29] J. Voiron, R. Ballou, J. Deportes, R. M. Galera, and E. Lelievre, J. Appl. Phys. **69**, 5678 (1991).
[30] R. Tanaka, S. Nakamichi, S. Endo, H. Wada, M. Shiga, and F. Ono, Solid State Commun. **78**, 489 (1991).
[31] S. Mondal, R. Cywinski, S. H. Kilcoyne, B. D. Rainford, and C. Ritter, Physica B **180&181**, 108 (1992).
[32] S. Endo, R. Tanaka, S. Nakamichi, F. Ono, H. Wada, and M. Shiga, J. Magn. Magn. Mater. **104-107**, 1441 (1992).
[33] R. A. Fisher, R. Ballou, J. P. Emerson, E. Levievre-Berna, N. E. Phillips, in *Proceedings of the International Conference on the Physics of Transition Metal '92*, edited by P. M. Oppeneer and J. Kübler (World Scientific, Singapore, 1993), p. 830.
[34] M. R. Ibarra, Z. Arnold, C. Marquina, L. Garcia-Orza, and A. del Moral, J. Magn. Magn. Mater. **128**, L249 (1993).
[35] M. R. Ibarra, Z. Arnold, C. Marquina, L. Garcia-Orza, and A. del Moral, J. Appl. Phys. **75**, 7158 (1994).
[36] R. Ballou, J. Deportes, R. Lemaire, P. Rouault, and J. L. Soubeyroux, J. Magn. Magn. Mater. **90&91**, 559 (1990).
[37] M. Shiga, J. Hirokawa, H. Wada, and Y. Nakamura, J. Phys. Soc. Jpn. **59**, 1410 (1990).
[38] T. Okamoto, H. Nagata, H. Fujii, and Y. Makihara, J. Magn. Magn. Mater. **70**, 139 (1987).
[39] J. Przewoźnik, J. Żukrowski, and K. Krop, J. Magn. Magn. Mater. **119**, 150 (1993).
[40] N. H. Kim-Ngan, P. E. Brommer, T. D. Hien, and J. J. Franse, Physica B **182**, 27 (1992).
[41] B. Coqblin, J. R. Iglesias-Sicardi, and R. Julien, Contemp. Phys. **19**, 327 (1978).
[42] A. Ponchet, J. M. Mignot, A. de Visser, J. J. Franse, and A. Menovsky, J. Magn. Magn. Mater. **54-57**, 399 (1986).
[43] M. S. Wire, J. D. Thompson, and Z. Fisk, Phys. Rev. B **30**, 5591 (1984).
[44] K. Kadowaki and S. B. Woods, Solid State Commun. **58**, 507 (1986).
[45] J. M. Fournier and E. Gratz, *Handbook on the Physics and Chemistry of Rare Earths*, edited by K. A. Gschneidner, Jr., L. Eyring, G. H. Lander, and G. R. Choppin (Elsevier Science Publishing, Amsterdam, 1993), Vol. 17, p. 409.
[46] R. J. Elliott and F. A. Wedgwood, Proc. Phys. Soc. London

81, 846 (1963).
[47] Nhu Hoa Kim-Ngan, Ph.D. thesis, Universiteit van Amsterdam, 1993.
[48] S. M. Jaakola and M. K. Hänninen, Solid State Commun. **36**, 275 (1980).
[49] G. Schütz (private communication).
[50] M. R. Ibarra, C. Marquina, L. Garcia-Orza, and A. del Moral, Solid State Commun. **87**, 695 (1993).
[51] M. R. Ibarra, L. Garcia-Orza, and A. del Moral, Solid State Commun. **84**, 875 (1992).
[52] M. R. Ibarra, C. Marquina, L. Garcia-Orza, Z. Arnold, and A. del Moral, J. Appl. Phys. **75**, 5662 (1994).
[53] S. K. Malik and W. E. Wallace, J. Magn. Magn. Mater. **24**, 23 (1981).
[54] T. Okamoto, H. Fujii, Y. Makihara, T. Hihara, and Y. Hashimoto, J. Magn. Magn. Mater. **54–57**, 1087 (1986).
[55] Y. Makihara, H. Fujii, K. Hiraoka, T. Kitai, and T. Hihara, J. Phys. (Paris) Colloq. Suppl. No. 12, **49**, C8-1087 (1988).